Role of Lys-226 in the Catalytic Mechanism of *Bacillus Stearothermophilus* Serine Hydroxymethyltransferase—Crystal Structure and Kinetic Studies[†,‡]

Siddegowda Bhavani,[||] V. Trivedi,[§] V. R. Jala,[||] H. S. Subramanya,[§] Purnima Kaul,[⊥] V. Prakash,[⊥] N. Appaji Rao,[||] and H. S. Savithri*[,||]

Department of Biochemistry, Indian Institute of Science, Bangalore, India, Molecular and Structural Biology Division, Central Drug Research Institute, Lucknow, India, and Protein Chemistry and Technology, Central Food Technology Research Institute, Mysore, India

Received October 14, 2004; Revised Manuscript Received March 17, 2005

ABSTRACT: Serine hydroxymethyltransferase (SHMT), a pyridoxal 5′-phosphate (PLP)-dependent enzyme catalyzes the reversible conversion of L-Ser and tetrahydropteroylglutamate (H_4PteGlu) to Gly and 5,10-methylene tetrahydropteroylglutamate (CH_2-H_4PteGlu). Biochemical and structural studies on this enzyme have implicated several residues in the catalytic mechanism, one of them being the active site lysine, which anchors PLP. It has been proposed that this residue is crucial for product expulsion. However, in other PLP-dependent enzymes, the corresponding residue has been implicated in the proton abstraction step of catalysis. In the present investigation, Lys-226 of *Bacillus stearothermophilus* SHMT (bsSHMT) was mutated to Met and Gln to evaluate the role of this residue in catalysis. The mutant enzymes contained 1 mol of PLP per mol of subunit suggesting that Schiff base formation with lysine is not essential for PLP binding. The 3D structure of the mutant enzymes revealed that PLP was bound at the active site in an orientation different from that of the wild-type enzyme. In the presence of substrate, the PLP ring was in an orientation superimposable with that of the external aldimine complex of wild-type enzyme. However, the mutant enzymes were inactive, and the kinetic analysis of the different steps of catalysis revealed that there was a drastic reduction in the rate of formation of the quinonoid intermediate. Analysis of these results along with the crystal structures suggested that K-226 is responsible for flipping of PLP from one orientation to another which is crucial for H_4PteGlu-dependent Cα−Cβ bond cleavage of L-Ser.

Serine hydroxymethyltransferase (SHMT)[1], a pyridoxal 5′-phosphate (PLP)-dependent enzyme belongs to the α-family (*1*) of PLP enzymes and catalyzes the reversible reaction of L-Ser and tetrahydropteroylglutamate (H_4PteGlu) to yield Gly and 5,10-methylene tetrahydropteroylglutamate (CH_2-H_4-PteGlu). SHMT is a key enzyme for the interconversion of the folate coenzymes and for the biosynthesis of purine, thymidine, and methionine. It is, therefore, postulated to be a target for cancer chemotherapy (*2*, *3*). The enzyme has been studied from several pro- and eukaryotic sources, and the properties have been reviewed (*4*−*6*).

Biochemical and structural studies on SHMT from various sources (*4*−*12*) have implicated several amino acid residues such as K-226, E-53, R-357, and H-122 in the catalytic mechanism of the enzyme (numbering according to the structure of *Bacillus stearothermophlus* serine hydroxymethyltransfarase (bsSHMT)) (*7*). The residues E-53 and H-122 have been implicated to participate in proton abstraction (*7*). However, mutational analysis of H-147 (corresponding to H-122) in sheep liver cytosolic SHMT (scSHMT) resulted only in a partial loss of activity, suggesting that this residue was probably not involved in the proton abstraction step of catalysis (*10*). The three-dimensional structure of the binary and ternary complexes of the bsSHMT (*7*) revealed that R-357 could interact with the carboxy group of L-Ser and E-53 was close to the hydroxymethyl group of L-Ser. Site-directed mutagenesis of R-363 in *Escherichia coli* (eSHMT) and R-401 in scSHMT (*11*, *12*) (corresponding to R-357 in bsSHMT) resulted in a complete loss of activity, confirming the role of this residue in substrate binding. On the basis of an analysis of these results, retroaldol cleavage and direct displacement mechanisms were proposed for the reaction catalyzed by SHMT (*3*, *7*). Recent observations of

[†] This study was supported by Department of Biotechnology, Government of India, New Delhi, India.

[‡] The coordinates have been deposited in the Protein Data Bank, as entries 1YJZ for K226M, 1YJY for K226M + Ser, and 1YJS for K226M + Gly.

* Correspondence should be addressed to Prof. H. S. Savithri, Department of Biochemistry, Indian Institute of Science, Bangalore, 560012, India. E-mail, bchss@biochem.iisc.ernet.in; Phone. + 91-80-23601561; fax, +91-80-23600814.

[||] Department of Biochemistry, Indian Institute of Science.

[§] Molecular and Structural Biology Division, Central Drug Research Institute.

[⊥] Protein Chemistry and Technology, Central Food Technology Research Institute.

[1] Abbreviations: AAT, aspartate aminotransferase; SHMT, serine hydroxymethyltransferase; scSHMT, sheep liver cytosolic SHMT; rcSHMT, rabbit cytosolic SHMT; eSHMT, *Escherchia coli* SHMT; bsHSMT, *Bacillus stearothermophilus* SHMT; mcSHMT, murine cytosolic SHMT; PLP, pyridoxal 5′-phosphate; MA, methoxyamine; 2-ME, 2-mercaptoethanol; DEAE-Cellulose, diethylaminoethyl cellulose; PteGlu, Folic Acid; H_4PteGlu, Tetrahydrofolate; CH_2-H_4Pte Glu, 5,10-methylene-H_4PteGlu; 5-CHO−H_4PteGlu, 5-formyl-H_4PteGlu; PMP, pyridoxamine-5′-phosphate; MPD, 2-methyl-2,4-pentanediol.

10.1021/bi047800x CCC: $30.25
Published on Web 04/16/2005

Scheme 1: Reaction Mechanism of bsSHMT with Serine and Glycine[a]

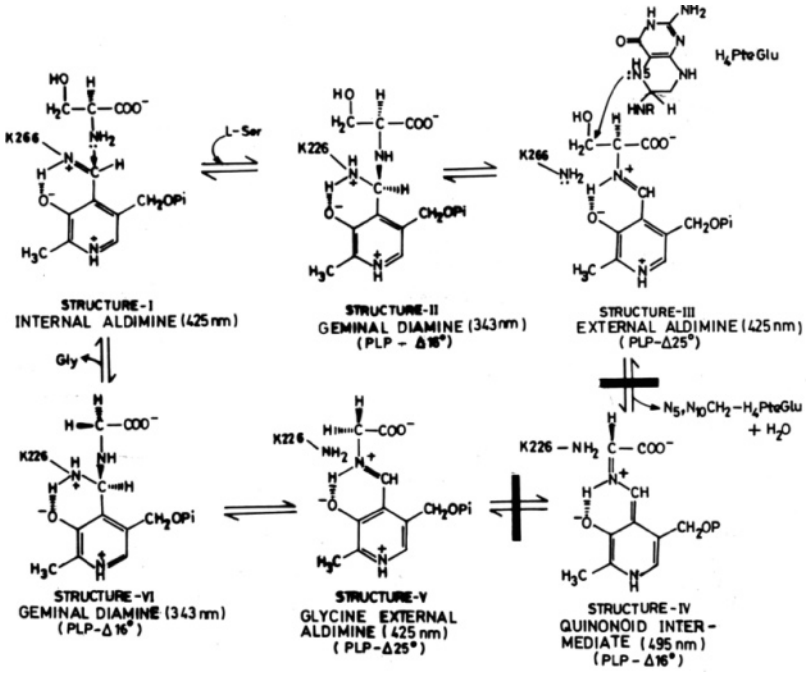

[a] bsSHMT was isolated as an internal aldimine with PLP linked to the ϵ-NH_2 group of K226 (structure I). The internal aldimine had an absorbance maximum at 425 nm. The internal aldimine upon reaction with L-Ser is converted to geminal diamine (structure II) absorbing at 343 nm. This conversion is accompanied by a change in the orientation of PLP by 16° from that in the internal aldimine form. The geminal diamine is then converted to external aldimine (structure III) where the bond with K-226 is broken. The orientation of PLP is changed by 25° from the initial orientation (in the internal aldimine, structure I) and by 9° from the geminal diamine (structure II). The attack of N_5 of H_4PteGlu on Cβ of L-Ser leads to bond cleavage resulting in the formation of quinonoid intermediate (structure IV), and the products 5,10-CH_2−H_4PteGlu and water are released. The orientation of the PLP ring returns back to that seen in the geminal diamine (16°) form, and the lysine residue is in close proximity to the product amino acid. The quinonoid intermediate is converted to the glycine external aldimine (structure V); the orientation of PLP in this intermediate is 25° from the initial point, which in turn is converted to the geminal diamine (with the change in orientation of PLP by 9°). The geminal diamine (structure VI) is converted to internal aldimine with the orientation of PLP returning to its initial position (structure I) upon interaction with K-226. The geminal diamine is converted to the internal aldimine (structure I) by the release of glycine. The internal aldimine is ready to catalyze the next cycle of reaction.

Szebenyi et al. (*9*) suggested that a combination of direct displacement and retroaldol cleavage could be a more probable mechanism (*9*).

The first step of the reaction (Scheme 1) involves conversion of the internal aldimine (structure I) upon addition of L-Ser to external aldimine (structure III) (via geminal diamine, structure II). The external aldimine is subsequently converted to a quinonoid intermediate as a result of a direct attack of N5 of H_4PteGlu on Cβ of serine, resulting in Cα−Cβ bond cleavage accompanied by release of a water molecule to form the product (glycine quinonoid intermediate); H_4PteGlu is converted to CH_2−H_4PteGlu (*7*). In the geminal diamine complex (structure II), the orientation of PLP is changed by 16° from that in the internal aldimine (structure I). Upon conversion to external aldimine (structure III) there is a further change in the orientation of 9° corresponding to a total change of 25° from that in the internal aldimine. The product quinonoid intermediate (in which the PLP is in an orientation similar to that of geminal diamine complex) is converted to Gly external aldimine, then to geminal aldimine, and finally, upon release of product Gly, the −CHO group of PLP interacts with the ϵ-NH_2 group of lysine to form the internal aldimine, and the PLP ring returns to its original orientation. It is observed that addition of H_4PteGlu results in the enhancement of proton abstraction from the Cα carbon and formation of quinonoid intermediate in the reverse reaction, that is, with glycine as substrate (Scheme 1).

Mutational analysis of the lysine residue, which anchors PLP, has been carried out in several PLP enzymes (*13*−*21*). The studies with aspartate aminotransferase (AAT) revealed that the mutant enzymes were either completely inactive or showed very low levels of activity depending on the nature of the substitutions of lysine. Mutation to Ala, Arg, or Cys resulted in an inactive enzyme (*13*, *16*, *17*), The His mutant had 0.1% activity compared to the wild-type enzyme (*16*). These observations were interpreted to suggest that the active site lysine amino group was serving as the base to remove the α-proton of the substrate in forming the quinonoid intermediate. This conclusion was also supported by the three-dimensional structure of the mutant enzymes (*19*).

On the other hand, *Escherichia coli* SHMT (eSHMT) K229H and K229R mutants were inactive, whereas the K229Q mutant was isolated with bound substrate and catalyzed a single turnover reaction (*20*). These results suggested that the Lys-229 was involved in the product expulsion step of catalysis. However, in the absence of crystal structure of these mutants and their substrate complexes, it is not possible to satisfactorily delineate the role of active site lysine residue in catalysis. The present paper describes the biochemical characterization of K226M and K226Q mutants of bsSHMT along with the three-dimensional structures in the unliganded and substrate-bound forms. An analysis of the results clearly suggested that lysine-226 plays a crucial role in H_4PteGlu-dependent Cα−Cβ bond cleavage

of serine and abstraction of Cα proton from glycine. The interaction of ϵ-NH_2 of K-226 with C4 of PLP is central for the flipping of PLP from one orientation to another among different enzyme intermediates, which is a crucial requirement in catalysis.

MATERIALS AND METHODS

Materials. L-[3-^{14}C]-Serine, restriction endonucleases, and DNA-modifying enzymes were obtained from Amersham Pharmacia Biotech Ltd., Buckinghamshire, England. Deep Vent Polymerase was purchased from New England Biolabs, Beverly, MO. Taq DNA polymerase was purchased from Bangalore Genei Pvt. Ltd., Bangalore. DEAE-Cellulose, Gly, L-Ser, D-Ala, 2-mercaptoethanol (2 -ME), folic acid, PLP, methoxyamine (MA), IPTG, and EDTA were obtained from Sigma Chemical Co., St. Louis, MO. Platinum oxide was purchased from Loba Chemie, Mumbai. All other chemicals used were of analytical reagent grade.

Bacterial Strains and Growth Conditions. E. coli strain DH5α (BRL) was the recipient for all the plasmids used in subcloning. The BL21 (DE3) pLysS strain (*22*) was used for bacterial expression of pRSH (*B. stearothermophilus* SHMT gene cloned and overexpressed in pRSET C vector) (*23*), and mutant constructs were similarly overexpressed. Luria−Bertani (LB) medium or terrific broth with 50 μg/mL of ampicillin was used for growing *E. coli* cells containing the plasmids (*24*).

DNA Manipulations. Plasmids were prepared by the alkaline lysis procedure (*24*). Preparation of competent cells and transformation were carried out by the method of Alexander (*25*). The DNA fragments were eluted with QIA quick gel extraction.

Site-Directed Mutagenesis. K226Q and K226M mutants of bsSHMT were constructed using the following primers: for K226Q, (sense primer) 5′GACGACGCATA*CAA*CG TTGCGC 3′ and (antisense primer) 5′ GCACAACGTTTGAT-GCGTCGTC 3′; for K226M, (sense primer) 5′ GACGACG-CAT*ATG*ACGTTGCGC 3′ and (antisense primer) 5′ GCG-CAACGTCATATGCGTCGT 3′. The nucleotides in italics indicate the mutations introduced. Primers were used on pRSH template to construct mutants by a PCR-based sense−antisense primer method (*23*). DNA sequencing, using ABI prism automated DNA sequencer, confirmed the presence of mutation and that no other mutations were present.

Expression and Purification of bsSHMT and Mutant Enzymes. The expression and purification of wild-type (bsSHMT) and the mutant enzymes were carried out essentially according to Jala et al. (*23*). Briefly, pRSH, K226M, and K226Q constructs were transformed into *E. coli* BL21 (DE3) pLysS strain. A single colony was grown in 50 mL of LB medium containing 50 μg/mL ampicillin at 30 °C. These cells were inoculated into 1 L of terrific broth medium containing 50 μg/mL ampicillin. After 3−4 h at 30 °C, cells were induced with 0.3 mM IPTG for 4−5 h. The cells were then harvested, re-suspended in 60 mL of buffer A (50 mM potassium phosphate buffer, pH 7.4, containing 2-ME, 1 mM EDTA, and 100 μM PLP), and sonicated. The supernatant was subjected to 0−65% ammonium sulfate precipitation; the pellet obtained was re-suspended in 20−30 mL of buffer B (20 mM potassium phosphate buffer, pH 8.0, containing 1 mM 2-ME, 1 mM EDTA, and 50 μM PLP) and dialyzed for 24 h against the same buffer (1 L with two changes). The dialyzed sample was loaded onto DEAE−cellulose, which was previously equilibrated with buffer B. The column was washed with 500 mL of buffer B, and the bound protein was eluted with 50 mL of buffer C (200 mM potassium phosphate buffer, pH 6.4, containing 1 mM EDTA, 1 mM 2-ME, and 50 μM PLP). The eluted protein was precipitated at 65% ammonium sulfate saturation, and the pellet was re-suspended in buffer D (50 mM potassium phosphate buffer, pH 7.4, containing 1 mM EDTA and 1 mM 2-ME) and dialyzed against the same buffer (2 L, with two changes) for 24 h. Protein was estimated using bovine serum albumin as a standard (*26*).

Enzyme Assays. Hydroxymethyltransferase Reaction. H_4-PteGlu-dependent cleavage of L-Ser to form Gly and 5,10-CH_2−H_4PteGlu was monitored using L-[3-^{14}C]-Ser and H_4PteGlu as substrates (*27*). One unit of enzyme activity was defined as the amount of the enzyme that catalyzes the formation of 1 μmol of formaldehyde/min at 37 °C. Specific activity was expressed as units per milligram of protein.

Transaminase Activity. H_4PteGlu-independent transamination of D-Ala yields pyruvate, and bound PLP is converted to pyridoxamine-5′-phosphate (PMP) (*28*). The spectra of bsSHMT, K226M, K226QbsSHMT (25 μM) in buffer D were recorded in a ShimadzuUV-160A spectrophotometer. Absorbance changes occurring at 425 nm upon addition of 100 mM D-Ala at 37 °C were recorded. The pseudo-first-order rate constants were calculated from these data. The reaction with D-Ala was used to prepare the wild-type and mutant apoenzymes. The enzyme concentration is always expressed in terms of subunit molecular weight.

Stopped-Flow Spectrophotometry. The pre-steady-state kinetics of the wild-type and the mutant bsSHMT with Gly or Gly + H_4PteGlu or methoxyamine (MA) were monitored, using SX.18MV-R stopped-flow spectrophotometer with a path length of 2 mm and pressure of 125 psi (8 bar), compressed nitrogen. The dead time of the instrument was 1 ms.

All experiments were performed in 50 mM potassium−phosphate buffer, (pH 7.4) containing 1 mM EDTA and 1 mM 2-ME. Single wavelength stopped-flow kinetic measurements were performed at 25 °C with temperature controlled by a circulating water bath. The mixer was set up with two syringes containing the enzyme (500 μM) and Gly (100 mM), or Gly + H_4PteGlu (70 μM) or MA (4 mM, 40 mM). The contents were mixed, and the reaction was initiated. Single wavelength data were collected at different time regimes. For each data set, 1000 data points were collected. All experiments were repeated at least three times for each of the time regimes. The data were analyzed using SX.18MV-R v4.42 software program (*29*, *30*).

Crystallization. Crystals of K226M and K226Q mutants were grown under the same conditions as described for the wild-type enzyme (*7*). In brief, crystals were obtained by mixing 4 μL of protein solution (375 μM) with 4 μL of reservoir solution containing 100 mM Hepes buffer, pH 7.5, 0.2 mM EDTA, 5 mM 2-ME, and 50% 2-methyl-2,4-pentanediol (MPD**)**. Crystals of complex of K226M with serine were grown under the same condition, except that the reservoir solution contained in addition 20 mM L-Ser. Crystals of K226Q complex with Gly were obtained under

Table 1: Statistics for Data Collection and Structure Determination of Lysine Mutants

	K226M	K226M + Ser	K226 + Gly
cell Dimensions (Å)	$a = 61.04$	$a = 61.98$	$a = 61.36$
	$b = 106.52$	$b = 106.27$	$b = 106.28$
	$c = 56.90$	$c = 56.89$	$c = 56.98$
resolution (Å)	2.1	2.25	2.00
completeness (all data) (%)	84.6	97.8	97.5
completeness (high resolution shell) (%)	89.1	98.0	97.5
R factor (high resolution shell) (%)	24.6	14.0	14.2
total reflections	128438	78324	203224
unique reflections	22373	18477	25927
final *R*-factor (all data) %	21.173	19.010	20.344
R_{free} (%)	26.087	22.701	22.863
rmsd (bonds) (Å)	0.013	0.013	0.011
rmsd (angles) (Å)	0.036	0.036	0.029
protein atoms	3116	3116	3116
substrate & cofactor atoms	15	22	20
water molecules	233	138	139

the same conditions except that the reservoir solution contained in addition 20 mM Gly and 100 μM PLP.

X-ray Diffraction Data Collection and Processing. For data collection, crystals were soaked for a few seconds in a harvesting solution containing 100 mM Hepes buffer, pH 7.5, 0.2 mM EDTA, 5 mM 2-ME, 30% MPD, and 25% glycerol and flash frozen in a nitrogen stream at 100 K. X-ray diffraction data were collected on a rotating anode X-ray generator using an image plate detector. The HKL program suite was used for data reduction and scaling (*31*). Crystals of both the mutants and their complexes belonged to $P2_12_12$ space group with one monomer in the asymmetric unit. Details of cell dimensions and data collection statistics for these crystals are shown in Table 1.

Structure Determination and Model Building. The bsSHMT (PDB code 1KKJ) crystal structure refined previously at 1.93 Å (*7*) was used as an initial model for the structure determination of K226M mutant crystals. The model was subjected to rigid body refinement using the program Xplor (*32*). The N- and C-terminal domains (residues 5−280 and 281−403) of the model were refined independently. Phases from this refined model were used to calculate $2F_o - F_c$ and $F_o - F_c$ maps and visualized using the graphics program Turbo-Frodo (*33*). The map was readily interpretable, and the electron density for the PLP cofactor, which was omitted from the model, was clearly visible. The model was further refined using maximum likelihood positional refinement in refmac, with restrained temperature factors. A manual model building was carried out using the program Turbo-Frodo (*34*). Solvent molecules were added during final cycles of refinement. The crystallographic free *R*-factor (*35*) was monitored at each stage to prevent model bias. Statistics of the final model are presented in Table 1.

The electron density maps for the K226M− L-Ser and K226Q−Gly complex crystals were computed using the structure of K226M protein as a model without PLP and solvent molecules. The models for the L-Ser- and Gly-bound mutant forms were subsequently refined in the same manner as the K226M mutant structure. Comparisons of the wild-type structures and mutant structures were carried out by manual superposition followed by rigid body refinement option in Turbo-Frodo, as well as using the CCP4 program lsqkab. Differences between the structures were detected visually and by calculating the distances between corresponding Cα atoms. The coordinates have been deposited in the Protein Data Bank, as entries 1YJZ for K226M, 1YJY for K226M + Ser, and 1YJS for K226M + Gly.

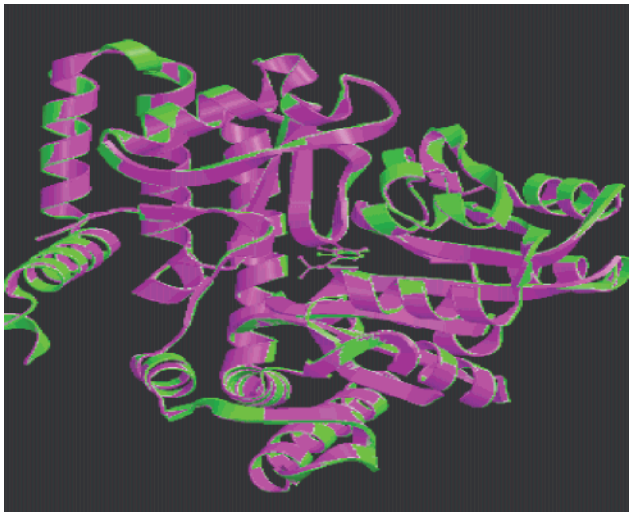

FIGURE 1: The crystal structures of bsSHMT and K226MbsSHMT. The structures of bsSHMT and K226MbsSHMT are shown as a ribbon diagram and overlaid on each other. The PLP molecule is shown in ball and stick representation. Color: bsSHMT in magenta and K226MbsSHMT in green. The coordinates have been deposited in the Protein Data Bank as entries 1YJZ for K226M, 1YJY for K226M + Ser, and 1YJS for K226M + Gly (an Identical pattern was obtained for K226QbsSHMT and is therefore not presented to avoid repetition).

RESULTS AND DISSCUSSION

Structure of Lysine Mutants of bsSHMT. The overall structures of the lysine mutants are very similar to that of the wild-type enzyme (Figure 1). K226M and K226QbsSHMT show a rms deviation of 0.14 Å and 0.15 Å, respectively, when compared with the wild-type enzyme. The mutation did not induce any gross conformational changes in the protein molecule. Active sites of both of the mutants are essentially similar to that of the wild-type enzyme. However, an interesting positional change was observed in the orientation of the PLP ring in the mutant protein structure compared to wild-type bsSHMT (Figure 2). The PLP ring in the mutant protein structure showed a rotation of approximately 16° around the C_5-C_5' bond of PLP (Figure 2), compared to the bsSHMT internal aldimine (*7*). The crystal structure of the ternary complex of murine cytosolic SHMT and bsSHMT showed a rotation of 16° of the PLP ring compared to the orientation of PLP in the internal aldimine (*7*, *36*). The orientation of PLP in these structures is ascribed to the position of PLP in the geminal diamine form. Similarly, structures of lysine mutants of AAT revealed a rotation of the PLP ring of 16° compared to the wild-type enzyme (*19*). The PLP ring in the structure of mutant protein with the substrate undergoes a further rotation of approximately 9° compared to the unliganded K226M and K226QbsSHMT structures. The conformation of the PLP ring in the structure of unliganded mutant SHMTs appears to be that of geminal diamine form, whereas the orientation of the PLP in the substrate-bound form of the mutant SHMTs appears to be in the external aldimine conformation, with a rotation of approximately 25° compared to the wild-type enzyme. The structures of the mutant enzymes clearly demonstrate that

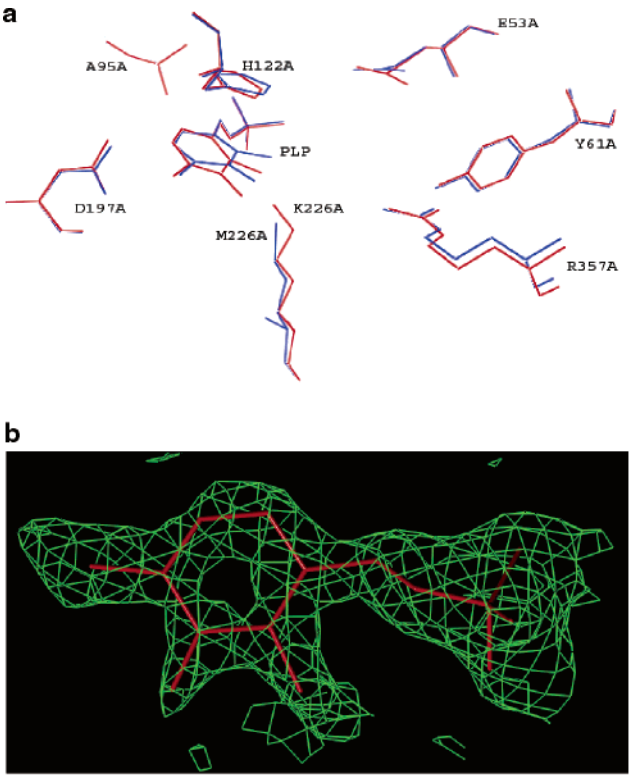

FIGURE 2: (a) Structure showing the change in orientation of the PLP ring. Color: The structure of bsSHMT in blue and K226M in red. (b) Electron density representing PLP in K226MbsSHMT.

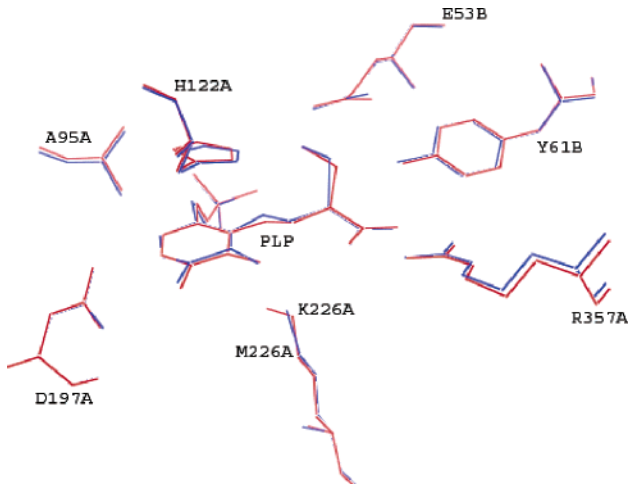

FIGURE 3: An overlay of serine external aldimine structures of bsSHMT and K226MbsSHMT. Color: bsSHMT serine external aldmine complex in red and K226MbsSHMT serine external aldimine complex in blue.

Table 2: Catalytic Activity and PLP Content of bsSHMT, K226M, and K226QbsSHMT

enzyme	activity[a]	activity after reduction[b]	PLP[c]	transaminase[d] (s^{-1})
Wt bsSHMT	5.2	0	1.0	0.040
K226MbsSHMT	0.023	0.0	1.0	0.021
K226QbsSHMT	0.021	0.0	0.5	0.015
			1.0	

[a] Micromol of HCHO per minute per milligram of protein. [b] Activity after reduction with $NaCNBH_3$. [c] One mole of PLP/mol of enzyme subunit assuming a value of ϵ of 6600 cm^{-1} M^{-1} at 388 nm for PLP. [d] Psuedo-first-order rate constant.

the PLP could bind even in the absence of a covalent bond with lysine (Figure 2). However, the orientation of the PLP ring seems to be affected by the disruption of the Schiff base.

On the basis of the spectral and kinetic studies of the lysine mutant of eSHMT (eK229Q), it has been reported that the enzyme was isolated with bound substrate (*20*). However, the lysine mutant structures of bsSHMT (Figure 2) clearly demonstrate that there was no density attributable to the bound substrate. The crystals of complexes of K226M and K226QbsSHMT with Ser/Gly were obtained by crystallization in the presence of 10 mM Ser/Gly in the drop (for details see Materials and Methods). The complexes (Ser/Gly) of the K226M and K226Q revealed the presence of the bound substrate in the active site of the enzyme. (Figure 3). The orientation of the PLP ring and the conformation of the substrate in the active site are very similar to that of external aldimine form of the wild-type enzyme. Thus, the formation of the external aldimine (Ser/Gly) from the PLP of the enzyme, which is in an orientation similar to that seen in geminal diamine complexes, seems to be unaffected by this mutation.

PLP Content and Catalytic Activity of Wild-Type and Lysine Mutants. The PLP content of K226MbsSHMT was 1 mol of PLP/mol of subunit, similar to that of the wild-type enzyme (Table 2), whereas K226QbsSHMT, as isolated, contained 0.5 mol of PLP/mol of subunit. Addition of 100 μM of PLP to this enzyme preparation, followed by incubation for 45 min at 4 °C and dialysis for 24 h against buffer not containing PLP, restored the PLP content to 1 mol of PLP/mol of subunit (Table 2). These observations suggest that PLP may not be as tightly bound in K226QbsSHMT compared to K226MbsSHMT (Table 2). This preparation of K226QbsSHMT containing 1 mol of PLP/mol of subunit was used throughout the studies. It is interesting to recall the observations with eSHMT lysine mutants, which are also dimers. K229QeSHMT was isolated with full complement of PLP but bound to the substrate, and K229HeSHMT did not contain PLP as external aldimine. In contrast, the mutation of Lys-256 in scSHMT resulted in the disruption of the tetrameric structure and loss of PLP (*21*). The specific activity of bsSHMT was 5.2 U/mg, whereas K226M and K226QbsSHMT, as isolated, had specific activities of 0.023 U/mg, and 0.021 U/mg, respectively, in the H_4PteGlu-dependent reaction with L-Ser. (Table 2). The wild-type and mutant enzyme preparations were treated with 0.4 mM $NaCNBH_3$, incubated for 30 min at 37 °C, and dialyzed overnight against 2 L of buffer D. This treatment reduces the internal aldimine to a secondary amine, whereas the external aldimine is not affected (*20*). bsSHMT lost all its activity, and the mutant enzymes also lost the residual activity, resulting in an enzyme preparation that was devoid of activity. When activity was assayed using a 10 000-fold excess of the mutant enzyme protein compared to wild-type enzyme, an insignificant amount of activity was found. Hence, the kinetic parameters such as K_m and k_{cat} of the mutant enzymes were not determined. These results suggest that mutation of Lys has resulted in a complete loss of activity. In the case of K229QeSHMT, the enzyme catalyzed a single turnover reaction but did not show steady-state catalytic activity. After a detailed examination, it was suggested that the Lys mutations in eSHMT had probably

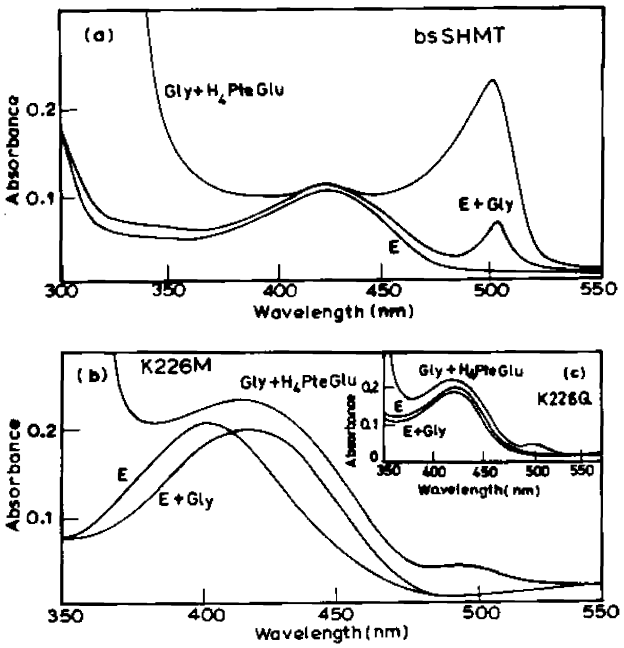

FIGURE 4: Absorbance changes on the addition of Gly and H_4-PteGlu to bsSHMT, K226MbsSHMT, and K226QbsSHMT. All spectra were recorded in Shimadzu UV-160 spectrophotometer at 20 ± 3 °C. All enzyme concentrations are expressed as mole per subunit. (a) The spectrum of bsSHMT (25 μM) gave an absorbance maximum at 425 nm characteristic for PLP internal aldimine (curve E). Addition of Gly (50 mM) gave a spectrum with a small peak at 495 nm, suggesting the formation of quinonoid intermediate (curve E + Gly). Further addition of H_4PteGlu (1.8 mM) enhanced the concentration of the quinonoid intermediate (curve Gly + H_4-PteGlu). (b) K226MbsSHMT (50 μM) gave a spectrum with an absorbance maximum at 412 nm (curve E); when Gly (50 mM) was added to the enzyme, the absorbance maximum shifted to 425 nm (curve E + Gly); when H_4PteGlu (when added to E + Gly) was added, a minor increase in absorbance at 495 nm was observed (curve Gly + H_4PteGlu). (c) Inset, similar experiments were carried out with K226MbsSHMT (50 μM). E represents K226QbsSHMT, and E + Gly and Gly + H_4PteGlu represent the spectrum obtained upon addition of Gly (50 mM), followed by H_4PteGlu.

affected the product release step of catalysis (*20*). Our results are in disagreement with this explanation as no detectable activity was observed with K226M and K226QbsSHMT (Table 2).

Spectral Properties and Kinetic Studies. K226MbsSHMT had an absorbance maximum at 412 nm compared to the absorbance maximum at 425 nm of the internal aldimine of bsSHMT (Figure 4). The 412 nm absorbance maximum for the K226MbsSHMT mutant could be due to the aldehyde from the PLP. The bathachromic shift from 390 to 412 nm could be due to altered interactions of the enzyme with PLP, especially in the absence of lysine residue. These altered interactions could be responsible for the change in the orientation of the PLP ring by 16° observed in the crystal structure of the mutant enzyme (Figure 2) compared to the internal aldimine structure of bsSHMT. It is interesting to recall that the active site lysine mutants of AAT also revealed a similar change in the orientation of the PLP ring (*19*). Addition of Gly to K226M and K226QbsSHMT resulted in a shift in the absorbance maximum from 412 to 425 nm, suggesting that PLP at the active site has the ability to react with the substrate and form an external aldimine complex (Figure 4). The orientations of the PLP ring and the amino

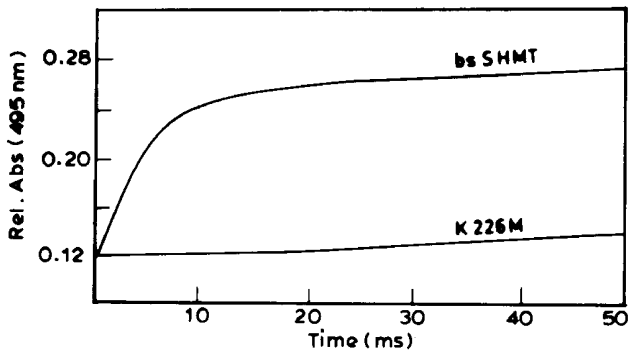

FIGURE 5: Kinetics of the formation of the quinonoid intermediate upon addition of H_4PteGlu to bsSHMT and K226M Gly complexes. Syringe A contained a mixture of bsSHMT (500 μM) + Gly (100 mM) incubated for 10 min at 18 °C and flowed against 70 μM of H_4PteGlu in syringe B. The relative absorbance at 495 nm was monitored in a stopped flow apparatus as described in Materials and Methods. A rapid increase in absorbance at 495 nm was monitored with bsSHMT. Whereas no change was observed with K226MbsSHMT, when a similar experiment was performed with K226QbsSHMT, no absorbance change was observed at 495 nm when the glycine complex was rapidly mixed with H_4PteGlu.

acid substrate in the crystal structure of the external aldimine forms of K226M and K226Q were very similar to their corresponding orientation in the external aldimine form of the wild-type enzyme (Figure 3).

In the reverse reaction with Gly, the conversion of Gly external aldimine to quinonoid intermediate occurs by the abstraction of a Cα proton (Scheme 1). Addition of Gly to wild-type bsSHMT resulted in a small increase in absorbance at 495 nm, indicating the formation of quinonoid intermediate (Figure 4), which was not seen in the mutants. The rate constant for the formation of the quinonoid intermediate with wild-type enzyme was 0.06 s^{-1}; however, this rate was not measurable for either of the mutants. Addition of H_4PteGlu to mutants resulted in the appearance of a very small peak (0.0567 au) at 495 nm, with a negligible rate constant. However, in the wild-type enzyme, addition of H_4PteGlu resulted in a large increase in the absorbance at 495 nm (0.234 au) (Figure 5) with a rate constant of 340 s^{-1} (measured using the stopped-flow apparatus as described in Materials and Methods). A similar increase in absorbance at 495 nm, upon addition of H_4PteGlu, was observed in all SHMTs (*4*, *5*). The absence of a considerable increase in absorbance at 495 nm, upon addition of Gly and H_4PteGlu, suggested that the H_4PteGlu-mediated proton abstraction was affected by mutation of K226 to Met or Gln.

5-CHO−H_4PteGlu, an analogue of H_4PteGlu, reacts with the quinonoid intermediate generated during the SHMT reaction with Gly (*37*). It can be seen from Figure 7 that the wild-type enzyme, upon interaction with glycine and 5-CHO−H_4PteGlu, yielded the characteristic quinonoid intermediate with a maximum absorbance at 495 nm, with a rate constant of 0.08 s^{-1}. The mutant enzyme did not show any absorbance change at 495 nm (Figure 6). These observations suggest that the quinonoid intermediate was not formed in the mutant with the substrates. It is possible that the conversion from structure V to structure IV (Scheme 1) does not occur in the mutant enzyme.

Hydroxylamine and its derivatives such as methoxyamine and aminoxyacetic acid have been used to monitor the reactivity of the internal aldimine of scSHMT (*12*). Earlier

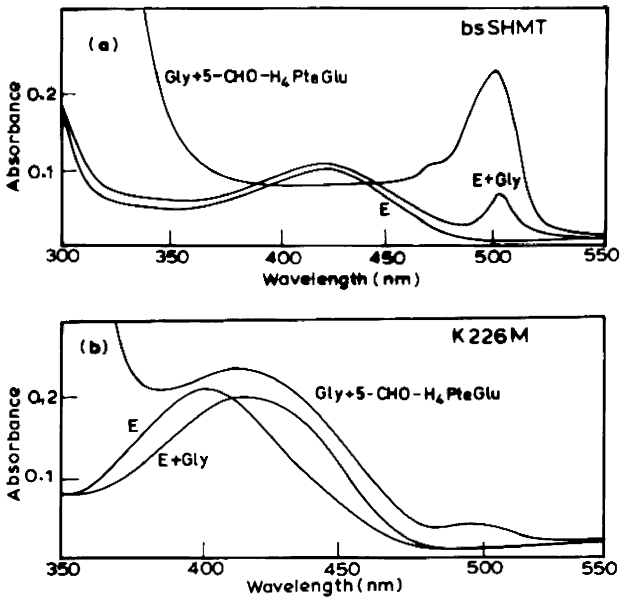

FIGURE 6: Interaction of 5-CHO−H_4PteGlu with bsSHMT and K226MbsSHMT. (a) bsSHMT (25 μM) was taken in buffer D, and the was spectrum recorded (curve E). To this solution, glycine (50 mM) was added and the spectrum recorded (curve E + Gly). 5-CHO−H_4PteGlu (70 μM) was added to the enzyme−Gly mixture, and the spectra was recorded (Gly + 5-CHO−H_4PteGlu), and the characteristic quinonid intermediate of the enzyme ternary complex was seen. (b) The spectrum of K226MbsSHMT (50 μM) was recorded as described above (curve E). Addition of glycine (50 mM) shifted the absorbance maximum from 412 to 425 nm. When 5-CHO−H_4PteGlu (70 μM) was added to the enzyme−glycine mixture, there was a hump at 495 nm (curve Gly + 5-CHO−H_4PteGlu.

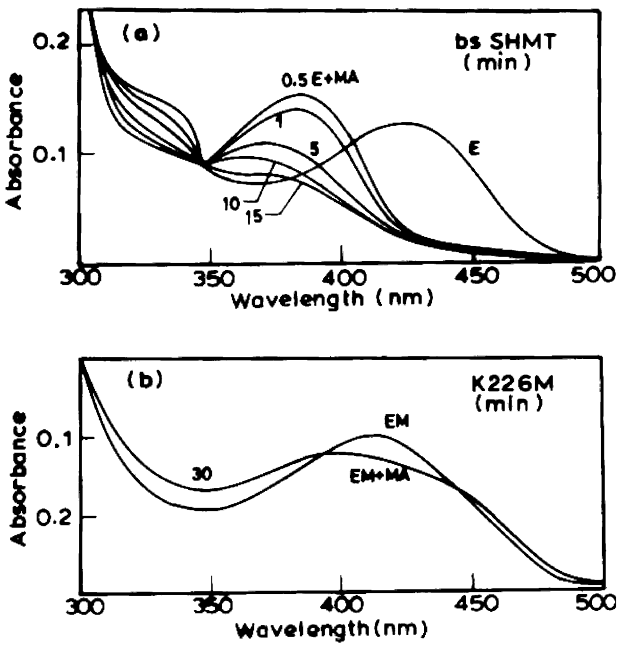

FIGURE 7: Interaction of Methoxyamine (MA) with bsSHMT and K226MbsSHMT. (a) To bsSHMT (25 μM), curve E, methoxyamine (2 mM) was added, and the spectra were recorded after 30 s, 5 min, 10 min, and 15 min. The figure shows the formation of an intermediate with absorbance maximum at 388 nm prior to formation of the product oxime absorbing at 325 nm. (b) The spectral changes observed in Figure 5a were not apparent when MA (10 mM) was added to K226MbsSHMT (25 μM). EM, K226MbsSHMT; EM + MA, K226MbsSHMT + MA.

observation on SHMT showed that methoxyamine reacts with the internal aldimine to generate a characteristic intermediate absorbing at 388 nm before the formation of the oxime product. (*30*) The interaction of methoxyamine with bsSHMT resulted in the disappearance of internal aldimine and Gly external aldimine at 425 nm and the formation of an intermediate with maximum absorbance at 388 nm (Figure 7). The rate of this reaction was monitored using stopped-flow kinetics. The rate constant was 1.6 s^{-1} for the disruption of the internal aldimine (as monitored by decrease in optical density at 425 nm) as well as for the formation of the intermediate (λ_{max} at 388 nm). The intermediate was converted to the oxime product with the absorbance maximum at 325 nm and a rate constant of 0.004 s^{-1} (Figure 6). Neither of the lysine mutants and their Gly external aldimine complexes showed any change in absorbance at 412, 388, and 325 nm indicating that PLP at the active site of the mutant was incapable of interacting with MA.

H_4PteGlu-Independent Reaction. In addition to the physiological reaction, SHMT catalyzes the H_4PteGlu-independent transamination of D-Ala to yield PMP and pyruvate as products. (*28*) The pseudo-first-order rate constants for transamination with D-Ala by K226M and K226QbsSHMT were 0.021 and 0.015 s^{-1}, respectively, compared to 0.04 s^{-1} for the wild-type enzyme (Table 2). This result suggests that mutation has not drastically affected the H_4PteGlu-independent activity. On the other hand, the H_4PteGlu-dependent physiological reaction is curtailed (Figure 4). It is interesting to recall that in the case of eSHMT, the H_4-PteGlu-independent activity of eK229R and eK229H was negligible (*20*), whereas K229QeSHMT showed considerable activity, similar to the observation with K226MbsSHMT (Table 2) (*20*). Transamination reaction has been extensively used to study the reversible binding of PLP at the active site. While PLP, in wild-type enzyme, could be removed in 1 h upon reaction with D-Ala, in the case of mutant bsSHMT, overnight (12 h) incubation was required to remove bound PLP. Addition of PLP to the apoenzymes resulted in regain of absorbance at 412 nm for the mutant enzyme and at 425 nm for apo-bsSHMT. Addition of substrate to the reconstituted apoenzyme of the mutant resulted in a shift in the absorbance maximum from 412 to 425 nm indicating the formation of external aldimine (data not presented). These results suggest that the mutation of the lysine residue has not affected the reversible binding of PLP to the enzyme, although the internal aldimine is not formed and the conversion of bound PLP to the external aldimine takes place readily upon the addition of Ser/Gly to K226M or K226QbsSHMT.

From the results presented in this paper, it is clear that, although the mutation of K226 does not affect the H_4PteGlu-independent reaction, it results in an almost complete loss of H_4PteGlu-dependent physiological reaction. This loss may not be due to the inability of the mutant to bind to H_4PteGlu. We were able to successfully model 5-CHO−H_4PteGlu into the structure of K226M and K226QbsSHMT substrate binary complexes, and H_4PteGlu binding pocket is unaffected. The fit was identical to that seen in the ternary complex of bsSHMT (data not shown).

This paper describes for the first time the crystal structure of lysine mutants of SHMT and their substrate complexes. In view of the lack of even a single turnover (Table 1) and

absence of bound H_2O at the active site (Figures 1, 2a, and 3), it can be suggested that K-226 plays a crucial role in an earlier step of catalysis (conversion of structure III to structure IV and structure V to structure IV). In order for the product to be formed, Cα−Cβ bond cleavage should be concurrent with the conversion of the enzyme from the external aldimine form of the substrate to the geminal aldimine form of the product (structure VI) prior to the release of the product and the formation of the internal aldimine (structure I). The orientation of PLP changes from 25° in the external aldimine form to 16° in the quinonoid intermediate, and the quinonoid intermediate is stabilized by the interactions of lysine at the active site (*36*). It is clear that the mutation does not affect either binding of PLP or its conversion to the substrate external aldimine complex (Table 2 and Figures 2, 3, and 4). However, the conversion of the external aldimine (PLP −25°) structure III to the quinonoid intermediate is affected (Figures 4 and 5). The quinonoid intermediate with the product Gly appears to be in the geminal diamine form (*36*). In the structure of the ternary complex of the mcSHMT as well bsSHMT (which are in quinonoid intermediate form), the PLP orientation is like that seen in geminal diamine complex.

In the absence of the ϵ-NH_2 group of lysine, the conversion of the external aldimine to product quinonoid intermediate, where the PLP orientation is similar to that of geminal diamine, that is, the change in orientation of PLP from 25° to 16°, may not be possible. This inturn could lead to shifting of equilibrium toward the substrate external aldimine form (serine form). Further, the interactions of K226 with residues such as Tyr-51 and Thr-223 have been implicated in the conversion of the enzyme from one form to another. (*7*, *38*). These interactions do not exist in K226MbsSHMT (Figures 2 and 3), and therefore, the conversion of substrate external aldimine to quinonoid intermediate (which is in an orientation similar to that of geminal diamine) is not possible. Thus K-226 is responsible for flipping of PLP from one orientation to another, which is accompanied by Cα−Cβ bond cleavage, and for the H_4PteGlu-mediated enhanced Cα proton abstraction in the reverse reaction.

ACKNOWLEDGMENT

We thank Prof. M. R. N. Murthy and Ms. Eaazhisai for her helpful discussions in the analysis of the X-ray structure data. We thank Dr. M. Ambili for providing the K226MbsSHMT clone.

REFERENCES

1. Mehta, P. K., and Christen, P. (2000) The molecular evolution of pyridoxal-5′-phosphate dependent enzymes, *Adv. Enzymol. Relat. Areas Mol. Biol. 74*, 129−84.
2. Appaji Rao, N., Talwar, R., Jagath, J. R., and Savithri, H. S. (2000) Tetrameric serine hydroxymethyltransferase: Insights into molecular organization, function and rational drug design, in *Supramolecular and Colloidal Structures in Biomaterials and Biosubstrates: Proceedings of the Fifth Royal Society-Unilever Indo-UK Forum* (Lal, M., Lillford, P. J., Naik, V. M., and Prakash, V., Eds.) pp 407−423, Imperial College Press, River Edge, NJ.
3. Matthews, R. B., and Drummond, J. T. (1990) Providing one-carbon units for biological methylations: Mechanistic studies on the serine hydroxymethyltransferase, methylenetetrahydrofolate reductase, and methlytetrahydrofolate-homocysteine methlytransferase, *Chem. Rev. 90*, 1275−1290.
4. Schirch, L. (1982) Serine hydroxymethyltransferase, *Adv. Enzymol. Relat. Areas Mol. Biol. 53*, 83−112.
5. Appaji Rao, N., Talwar, R., and Savithri, H. S. (2000) Molecular organization, catalytic mechanism and function of serine hydroxymethyltransferase—a potential target for cancer chemotherapy, *Int. J. Biochem. Cell. Biol. 32*, 405−416.
6. Appaji Rao, N., Ambili, M., Jala, V. R., Subramanya, H. S., and Savithri, H. S. (2003) Structure−function relationship in serine hydroxymethyltransferase, *Biochem. Biophys. Acta 1647*, 24−29.
7. Trivedi, V., Gupta, A., Jala, V. R., Saravanan, P., Rao, G. S. J., Appaji Rao, N., Savithri, H. S., and Subramanya, H. S. (2002) Crystal structure of binary and ternary complexes of serine hydroxymethyltransferase from *Bacillus stearothermophilus*: Insights into the catalytic mechanism, *J. Biol. Chem. 227*, 17161−17169.
8. Krishna Rao, J. V., Prakash, V., Appaji Rao, N., and Savithri, H. S. (2000) The role of Glu74 and Tyr82 in the reaction catalyzed by sheep liver cytosolic serine hydroxymethyltransferase, *Eur. J. Biochem. 267*, 5967−5976.
9. Szebenyi, D. M. E., Musayev, F. N., di Salvo, M. L., Safo, M. K., and Schirch, V. (2004) Serine hydroxymethyltransferase: Role of Glu75 and evidence that serine is cleaved by a retroaldol mechanism, *Biochemistry 43*, 6865−6876.
10. Jagath, J. R., Sharma, B., Appaji Rao, N., and Savithri, H. S. (1997) The role of His-134, 147 and 150 residues in subunit assembly, cofactor binding and catalysis of sheep liver of cytosolic serine hydroxymethyltransferase, *J. Biol. Chem. 272*, 24355−24362.
11. Delle Fratte S., Iurescia, S., Angelaccio, S., Bossa, F., and Schirch, V. (1994) The function of arginine 363 at the substrate carboxyl binding site in *Escherichia coli* serine hydroxymethyltransferase, *Eur. J. Biochem. 225*, 395−401.
12. Jagath, J. R., Appaji Rao, N., and Savithri, H. S. (1997) Role of Arg - 401 of cytosolic serine hydroxymethyltransferase in subunit assembly and interaction with the substrate carboxyl group, *Biochem. J. 327*, 877−882.
13. Malcom, B. A., and Kirsch, J. F. (1985) Site-directed mutagenesis of aspartate aminotransferase from *Escherichia coli*, *Biochem. Biophys. Res. Commun. 132*, 915−921.
14. Kirsch, J. F., Finlayson, W. L., Toney, M. D., and Cronin, C. N. (1987) Mechanistic analysis of the aspartate aminotransferase active site mutants—Y70F, K258A, and R292D, in *Biochemistry of Vitamin B_6: Proceedings of the 7th International Congress on Chemical and Biological Aspects of Vitamin B_6 Catalysis* (Korpela, T., and Christen, P., Eds.) p 59, Birkhaeuser, Basel, Switzerland.
15. Toney, M. D. and Kirsch, J. F. (1989) Direct Brønsted analysis of the restoration of activity to a mutant enzyme by exogenous amine, *Science, 243*, 1485.
16. Ziak, M., Jaussi, R., Gehring, H., and Christen, P. (1990) Aspartate aminotransferase with the pyridoxal-5′-phosphate-binding lysine residue replaced by histidine retains partial catalytic competence, *Eur. J. Biochem. 181*, 329−333.
17. Toney, M. D., and Kirsch, J. F. (1991) The K258R mutant of aspartate aminotransferase stabilizes the quinonoid intermediate, *J. Biol. Chem. 266*, 23900−23903.
18. Kirsch, J. F., Planas, A., and Toney, M. D. (1991) Genetic engineering and chemical modification at the position of lysine 258 in aspartate aminotransferase, in *Enzymes Dependent on Pyridoxal Phosphate and Other Carbonyl Compounds as Cofactors* (Fukui, K., Kagamiyama, H., Soda, K., and Wada, H., Eds.) pp 161−167, Pergamon Press, Oxford, England.
19. Malashkevich, V. N., Jager, J., Zaik, M., Sauder, U., Gehring, H., Christen, P., and Jansonius, J. N. (1995) Structural basis for the catalytic activity of aspartate aminotransferase K258H lacking the pyridoxal-5′-phosphate-binding lysine residue, *Biochemistry 34*, 405−414.
20. Schirch, D., Delle Frattes, S., Iurescia, S., Angelaccio, S., Contestabiles, R., Bossa, F., and Schirch, V. (1993) Function of active-site lysine in *Escherichia coli* serine hydroxymethyltransferase, *J. Biol. Chem. 268*, 23132−23138.
21. Talwar, R., Jagath, J. R., Datta, A., Prakash, V., Savithri, H. S., and Appaji Rao, N. (1997) The role of lysine-256 in the structure and function of sheep liver recombinant serine hydroxymethyltransferase, *Acta Biochim. Pol. 44*, 679−688.
22. Studier, F. W., and Moffat, B. A. (1986) Use of bacteriophage T7 RNA polymerase to direct selective high expression of cloned genes, *J. Mol. Biol. 189*, 113−130.
23. Jala, V. R., Prakash, V., Appaji Rao, N., and Savithri, H. S. (2002) Over expression and characterization of dimeric and tetrameric forms of recombinant serine hydroxymethyltransferase from *Bacillus stearothermophilus*, *J. Biosci. 27*, 233−42.

24. Sambrook, J., Fritsch, E. F., and Maniatis, T. (1989) *Molecular Cloning: A Laboratory Manual*, 2nd ed., Cold Spring Harbor Laboratory, Cold Spring Harbor, NY.
25. Alexander, D. C. (1987) An efficient vector-primer cDNA cloning system: Large scale preparation of competent cells, *Methods Enzymol. 154*, 41−64.
26. Lowry, O. H., Rosebrough, N. J., Farr, A. L., and Randall, R. J. (1951) Protein measurement with the folin phenol reagent, *J. Biol. Chem. 193*, 265−275.
27. Taylor, R. T., and Weissbach, H. (1965) A radioactive assay for serine hydroxymethyltransferase, *Anal. Biochem. 13*, 80−84.
28. Schirch, V., and Jenkins, W. T. (1964) Serine transhydroxymethylase-transamination of D-alanine, *J. Biol. Chem.* 239, 3797−3800.
29. Baskaran, N., Prakash, V., Appu Rao, A. G., Radhakrishnan, A. N., Savithri, H. S., and Appaji Rao, N. (1989) Mechanism of interaction of *O*-amino-D-serine with sheep liver serine hydroxymethyltransferase, *Biochemistry, 28*, 9607−9612.
30. Acharya, J. K., Prakash, V., Rao, A. G., Savithri, H. S., and Appaji Rao, N. (1991) Interactions of methoxyamine with pyridoxal-5′-phosphate-Schiff's base at the active site of sheep liver serine-hydroxymethyltransferase, *Indian J. Biochem. Biophys. 28*, 381−388.
31. Otowinski, Z., and Minor, W. (1997) Processing of X-ray diffraction data collected in oscillation mode, *Methods Enzymol. 276*, 307−326.
32. Brunger, A. T., Karplus, M., and Petsko, G. A. (1989) Crystallographic refinement by simulated annealing: Application to crambin, *Acta Crystallogr., Sect. A 45*, 50−61.
33. Roussel, A., and Cambillau, C. (1989) In *Silicon Graphics Geometry Partner Directory*, pp 77−78, Silicon Graphics, Mountain View, CA.
34. Murshudov, G. N., Vagin, A. A., and Dodson, E. J. (1997) Refinement of macromolecular structures by the maximum-likelihood method, *Acta Crystallogr. D53*, 240−245.
35. Brunger, A. T. (1992) Free R value: A novel statistical quantity for assessing the accuracy of crystal structures, *Nature 355*, 472−474.
36. Szebenyi, D. M., E., Liu., X., Kriksunov, I. A., Stover, P. J., and Thiel, D. J. (2000) Structure of a murine cytoplasmic serine hydroxymethyltransferase quinonoid ternary complex: Evidence for asymmetric obligate dimers, *Biochemistry 39*, 13313−13323.
37. Stover, P., and Schirch, V. (1991) 5-Formyltetrahydrofolate polyglutamates are slow binding inhibitors of serine hydroxymethyltransferase, *J. Biol. Chem. 226*, 1543−1550.
38. Angelaccio, S., Pascarella, S., Fattori, E., Bossa, F., Strong, W., and Schirch, V. (1992) Serine hydroxymethyltransfease: Origin of substrate specificity, *Biochemistry 31*, 155−162.

BI047800X